

SPUTTERING OF COPPER BY HYDROGEN IONS WITH ENERGIES UP TO 50 keV

N. V. PLESHIVTSEV

Institute of Chemical Physics, Academy of Sciences, U.S.S.R.

Submitted to JETP editor June 10, 1959

J. Exptl. Theoret. Phys. (U.S.S.R.) 37, 1233-1240 (November, 1959)

The dependence of the sputtering ratio S (atoms/ion) on energy, angle of incidence, and mean ion current density was investigated by means of an ion gun. The angular distribution of sputtered particles and the microrelief of the surface were also studied. $S \sim (\ln E)/E$ was found for ion energies $E = 15 - 55$ keV. The sputtering ratio grows with increase of the angle of incidence and within a certain range is independent of the mean beam current density. For both normal and oblique beam incidence the angular distribution of sputtered particles differs significantly from a cosine law. Grooves are formed along the direction of incidence when the beam strikes the surface at an oblique angle. The data indicate that at intermediate energies momentum transfer plays the most important part in the elementary sputtering act.

INTRODUCTION

IN several recent investigations¹⁻¹¹ cathode sputtering has been studied by means of an ion beam instead of a gas discharge. Heavy ions were used for the most part to study the dependence of the sputtering ratio on ion energy and mass^{1-5,8,11} and on target temperature,⁷ as well as to study the mass and velocity spectra of the sputtered particles¹⁰ and their angular distribution.¹¹ Most of the investigations were performed with low-energy heavy ions, but in a few instances^{2,8,11} the energy was carried to 25 - 30 keV. However, in some electric vacuum devices, experimental apparatus and accelerators light ions are employed with energies measured in tens of keV or in MeV. In such cases sputtering is accompanied by many undesired effects which must be suppressed. Information concerning sputtering by light ions has been limited to energies up to 2 keV. The sputtering of copper by hydrogen ions of 10 - 50 keV and higher is therefore of decided interest.

1. EXPERIMENTAL TECHNIQUE

The experimental apparatus is shown schematically in Fig. 1. The hydrogen ion beam was produced by an ion gun containing a source with a doubly-confined plasma.^{12,13} Commercially pure hydrogen passed through the walls of a heated nickel tube into the gas-discharge chamber of the source. After ionization in an arc from a hot cathode, in an inhomogeneous magnetic field, the hydrogen ions were drawn from the chamber, and were

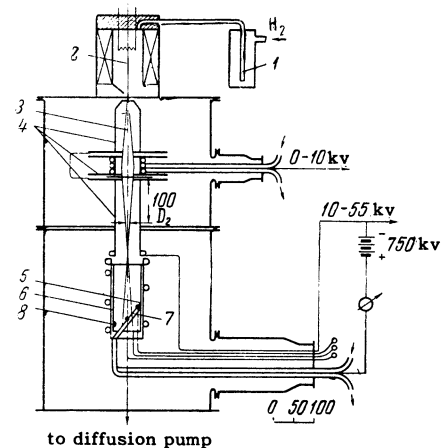
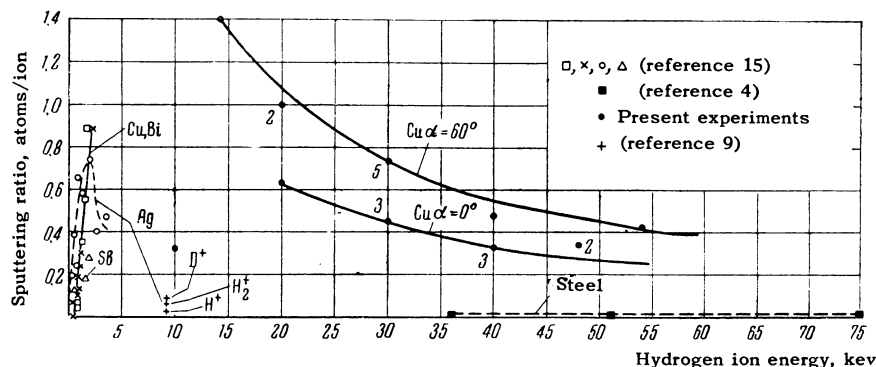


FIG. 1. Diagram of apparatus. 1 - nickel diffusion leak, 2 - ion source, 3 - ion beam, 4 - electrodes of univoltage electrostatic lens, 5 - target for angle of incidence $\alpha = 60^\circ$, 6 - Faraday cup, 7 - copper-kopel thermocouples, 8 - collector of sputtered copper.

then focused and accelerated by a univoltage (symmetrical) electrostatic lens. The accelerating potential was measured by a class-1.5 electrostatic kilovoltmeter.

The ion gun produced hydrogen ion beams with currents up to 30 ma at $U = 55$ keV. However, smaller currents of 3 - 10 ma were used in order to keep the beam from striking and consequently sputtering the lens electrodes. The ion beam was observed distinctly and measured visually by means of the radiation from excited and recombining atoms, through openings in the electrodes. Difficulties of experimental design prevented a mass-spectrographic analysis of the beam, since a high voltage

FIG. 2. Sputtering ratio as a function of hydrogen ion energy and angle of incidence. The numerals on the curves indicate the number of experimental runs.



was applied to the Faraday cup, which was followed directly by the vacuum apparatus. In order to maintain a beam of constant composition the source was operated under steady conditions. The arc voltage and current were 100 v and 0.5 amp; the pressure was 3×10^{-2} mm Hg; the current in the constraining magnetic coil was 2 amp.

The number of ions striking the target was measured calorimetrically since electric measurements by means of a cutoff potential give current values which are often too high by a factor of 3 or 4. Inlet and outlet temperatures of the target-cooling water were measured by thermocouples with 1°C scale divisions, with a consequent error of 10–25%.

The targets varied in design. At angle of incidence $\alpha = 0^\circ$ the target was usually a copper disk 70 mm in diameter and 2–4 mm thick, to one side of which three thermocouples were attached. This surface was cooled by water. The target used at $\alpha = 60^\circ$ was an ellipse 1 mm thick produced by a 60° intersection of a plane with a cylinder 70 mm in diameter. A cooling tube was soldered to the target perimeter and three thermocouples were also attached in this instance. The target surfaces were washed in alcohol before the first experiment and were subjected to no further treatment.

The collectors of sputtered copper were made of $260 \times 200 \times 0.1$ mm nickel foil held by two snap rings against the inside surface of a water-cooled Faraday cup 80 mm in diameter.

The quantity of sputtered copper was determined from the changes of target and collector weights, using an ADV-200 analytical balance for double weighing to eliminate random errors. The weighing was accurate to within 0.1 or 0.2 mg. In some instances an assay balance accurate to within 0.02 mg was used. The sputtered material weighed from 3 to 35 mg.

The experimental error is estimated at 15–30% depending on the beam energy. The sputtering ratio was calculated by means of the formula

$$S = 1.5 m / Q,$$

where m is the weight of sputtered copper in milligrams and Q is the quantity of ions striking the target measured in coulombs.

The vacuum for the ion gun was produced by a 1000-liter oil diffusion pump with a standard water trap. A vacuum of 6×10^{-6} mm Hg was attained, while the working pressure was $3 - 5 \times 10^{-5}$ mm Hg according to a LM-2 air gauge, or $1 - 2 \times 10^{-5}$ mm Hg when converted to hydrogen.

Measurements of the several experimental parameters (ion current, accelerating voltage, target temperature, pressure etc.) were obtained in 5–10 minutes, with a single measurement requiring 5 minutes.

2. DEPENDENCE OF SPUTTERING RATIO ON ION ENERGY; ANGLE OF INCIDENCE AND MEAN CURRENT DENSITY

The sputtering of metals by hydrogen and deuterium ions has not been investigated very thoroughly. The available data are shown in Fig. 2. Guntherschulze and Meyer obtained data on copper sputtering in a gas discharge for the energy range 0.3–2 keV.¹⁵

When an ion beam interacts with a metal surface residual gas molecules may form surface films of different colors and shades (black or blue). A similar effect, which is probably polymerization, is produced by electron bombardment of specimens in electron microscopes. Investigations of this phenomenon are reported in reference 16. Experiments on copper sputtering using an ion gun (10–55 keV) and in an accelerator tube (300–600 keV) provide a basis for a few remarks concerning the building up of such films. The formation of a film depends on the ion current density, sputtering ratio, and target temperature and on the presence of a diaphragm in the path of the beam. With 20–600 keV ion energies at normal incidence, when the copper surface temperature is 50–100°C a film is not formed if the density of H_2^+ or D_2^+ exceeds 0.5–1.5 ma/cm². At $\alpha = 60^\circ$ with H_2^+ ions of 15–55 keV and the

Data from experiments to determine the sputtering ratio as a function of ion energy and angle of incidence

No. of experiment	Ion energy, kev	Ion current, ma	Mean ion current density, ma/cm ²	Target temperature, °C	Quantity of ions, Q, coulombs	Weight of copper on collector, mg	Decrease of target weight, mg	Correction for ion weight, mg	Weight of sputtered copper, mg	Sputtering ratio, Cu atoms/ion
Angle of incidence $\alpha = 0^\circ$										
23	10	1.5	0.2	25	12.5	3.0	2.1	0.2	2.3	0.28—0.36
5	20	5.0	0.2	550	55	—	36.6	0.8	37.4	1.04
6	20	5.2	0.2	650	27.5	—	11.5	0.4	11.9	0.65
1	30	8.6	0.45	250	100	—	23.0	1.5	24.5	0.37
7	29	10.0	0.6	80	50	—	18.3	0.75	19.1	0.57
8	29	9.3	1.1	80	93	—	23.4	1.4	24.8	0.40
2	39	7.7	0.4	250	67	—	13	1.0	14.0	0.31
4	40	6.2	0.9	400	15	—	3.7	0.25	4.0	0.40
9	40	10.5	0.8	80	12.5	—	15.8	1.9	17.7	0.21
20	48	4.5	1.6	100	16.7	3.5	4.2	0.25	4.5	0.40—0.31
21	49	9.3	1.3	100	75	9.4	16.4	1.1	17.5	0.35—0.19
Angle of incidence $\alpha = 60^\circ$										
13	14	3.0	0.07	60	15.1	14	13.0	0.2	13.2	1.30—1.40
14	20	5.3	0.13	80	19.0	11.9	21.2	0.3	21.5	1.7—1.0
11	21	5.1	0.18	40	23.0	—	16.2	0.35	16.6	1.1
12	26	7.0	0.22	100	31.5	—	12.1	0.5	12.6	0.60
16	30	5.6	0.30	100	20.1	7.2	10.4	0.3	10.7	0.80—0.54
17	30	5.7	0.16	100	20.5	8.3	9.7	0.3	10.0	0.73—0.61
18	30	5.8	0.22	100	21.0	7.4	9.3	0.3	9.6	0.69—0.53
10	31	6.9	0.23	100	20.7	—	10.6	0.3	10.9	0.80
15	32	7.0	0.26	150	29.5	13.3	15.3	0.45	15.8	0.81—0.68
19	40	5.7	0.21	150	42.2	6.3	13.0	0.65	13.7	0.49—0.23
22	54	7.3	0.42	240	55.0	16.0	34.4	0.80	35.2	0.96—0.44

same temperature range a film is not formed with 0.2—0.4 ma/cm². Diaphragm apertures in the beam path assist the production of films, which do not appear, however, when the target temperature exceeds 400—450°C. The longest experiment yielded ~0.5 mg as the weight of the film at the periphery of the spot burned by the beam.

The experimental conditions and results are given in the table. In most instances the weight of sputtered copper leaving the target was approximately equal to the weight of the copper deposited on the collector. Figure 2 shows the sputtering ratio as a function of energy and angle of incidence. S as a function of energy is quite well approximated by the relation $S \sim (\ln E)/E$, where E is the ion energy.

In experiments 1 and 2 it was established by means of a divided target consisting of nine copper foils that the radial distribution of beam current density can be represented by a Gaussian error

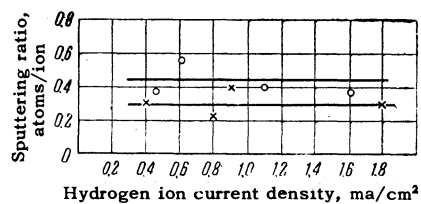


FIG. 3. Sputtering ratio as a function of ion current density ($\alpha = 0^\circ$), o — $E = 30$ keV, $T = 80$ — 250°C ; x — $E = 40$ keV, $T = 80$ — 400°C

curve. Therefore the column for "Mean ion current density" in the table gives the total current to the target divided by the area of the beam spot. Figure 3 shows the relation between S and the mean ion current density.

3. ANGULAR DISTRIBUTION OF SPUTTERED PARTICLES

The angular distribution of sputtered particles was investigated by Seeliger and Sommermeyer,¹⁷ who were the first to use ion beams to study cathode sputtering. When silver and gallium were bombarded at $\alpha \leq 45^\circ$ by argon ions with 5—10 keV a cosine-law angular distribution of the sputtered particles was observed. Guntherschulze¹⁸ observed a departure from the cosine law in the sputtering of silver by hydrogen ions with 0.5—3 keV. A departure from the cosine law was also reported in reference 11.

For the purpose of studying the angular distribution at $\alpha = 60^\circ$, 14 nickel foils of dimensions $20 \times 20 \times 0.1$ mm³ were attached to the nickel collecting cylinder (Fig. 4). These were weighed to within 0.02 mg. The experimental results are represented in Figs 4a and 4b, where the numerals inside the squares denote the identifying numbers of the collecting foils and the quantity of sputtered

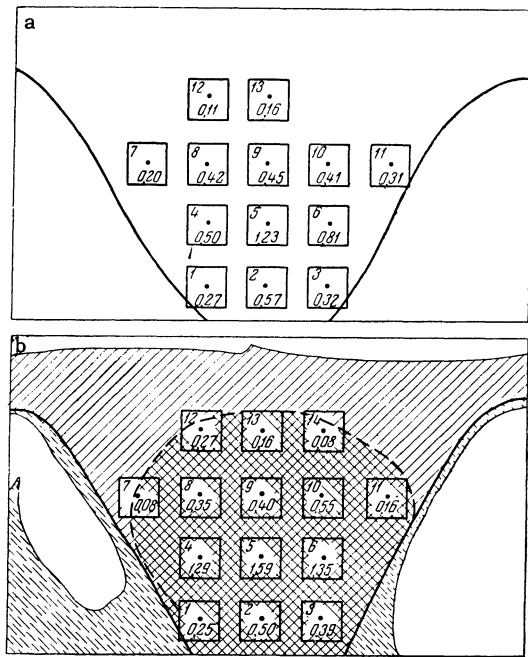


FIG. 4. Distribution of sputtered copper on square collecting foils ($\alpha = 60^\circ$), a — $E = 40$ keV, $T = 150^\circ\text{C}$; b — $E = 54$ keV, $T = 240^\circ\text{C}$.

copper in milligrams. In Fig. 4b the bright spot of deposited copper is represented by crosshatching. The distribution of sputtered copper at $\alpha = 0^\circ$ was studied by means of strips attached parallel to the Faraday cylinder axis. Figure 5a — d shows the angular distributions of copper for $\alpha = 60^\circ$ and $\alpha = 0^\circ$, which in all cases deviate considerably from a cosine law. This is especially marked in the case of 54-keV ions. In this case, at $\alpha = 60^\circ$, the angular distribution peak is shifted from the normal to the target by approximately half the angle of incidence.

4. SURFACE CONDITION

After each experiment it was almost always possible to observe four clearly defined regions. The granular structure at the center of the beam spot was visible even with the naked eye. After prolonged bombardment the copper begins to flake off in this area; strong etching separates the grains from the surface. The second region, which is a ring around the center, has the bright red color of reduced copper. The next ring is light red in color, while the peripheral region is covered with a translucent dark film. These regions result from the nonuniform lateral distribution of current density.

The targets were studied and photographed using a MS-51 comparator and a MIM-6 metallurgical microscope. Targets which were bombarded at

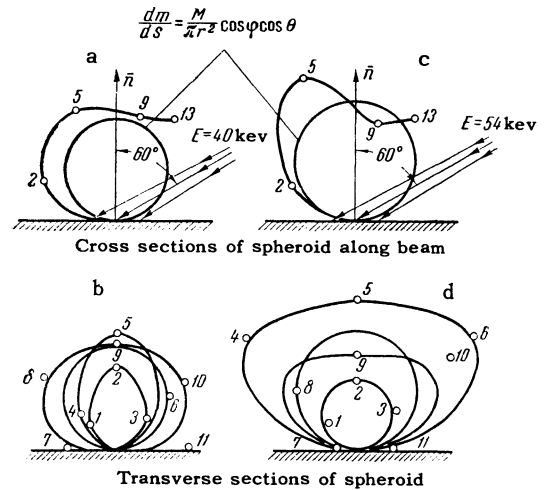


FIG. 5. Angular distribution of sputtered copper. a, b — $E = 40$ keV, $\alpha = 60^\circ$, $T = 150^\circ\text{C}$; c, d — $E = 54$ keV, $\alpha = 60^\circ$, $T = 240^\circ\text{C}$; e — $E = 49$ keV, $\alpha = 0^\circ$, $T = 100^\circ\text{C}$. The numerals on the curves denote the collecting foils as shown in Fig. 4.

$\alpha = 0^\circ$ clearly showed the usual etch figures, cones and pits* (Fig. 6a). The numbers of cones and depressions increase with the ion current density. Estimates based on the sharpness of focusing and resolution of the microscope gave a cone vertex diameter of $\sim 3 \mu$ and height $\sim 30 \mu$. Targets positioned at 30° with respect to the beam exhibited grooves $\sim 5 \mu$ wide and $\sim 30 \mu$ long instead of cones and pits (Fig. 6b). The grooves indicate the direction of beam incidence and increase in number toward the beam center.

5. DISCUSSION OF RESULTS

The reduction of the sputtering ratio with increasing energy† can be accounted for by several

*The presence of pits was pointed out to the author by V. E. Yurasova.

† Indirect confirmation of this relationship can be found in the data obtained by B. V. Panin for the behavior of the ion-ion emission ratio, where a peak is observed at 8–10 keV (private communication), and also in reference 11.



a



b

FIG. 6. Microrelief of copper surface after sputtering by hydrogen ions ($\times 130$); a - $E = 30$ keV, $j = 1.6$ ma/cm², $t = 194$ min; b - $E = 14-54$ keV, $j = 0.07-0.8$ ma/cm², $t = 842$ min.

factors, principally 1) increased ion range in the target material and the resulting greater depth from which the diffusion or ejection of displaced atoms occurs; 2) increased ion energy loss due to ionization and excitation in the region where the ion velocity is approximately equal to the velocity of orbital electrons. The sputtering curve peak was predicted by Keywell⁵ while the monotonic decline following a $(\ln E)/E$ law was derived by Goldman and Simon¹⁹ for ion energies above 50 keV.

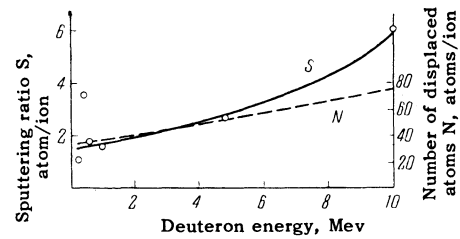


FIG. 7. Comparison of the number of displaced copper atoms with the number of sputtered atoms produced by deuterons with energies of 0.3–10 MeV.

Preliminary results for copper sputtering by 300 – 600 keV deuterons and in a cyclotron at 1 – 10 MeV indicated that the sputtering ratio increases with energy (Fig. 7). These data show that the theory of Goldman and Simon¹⁹ for deuteron energies above 300 keV leads to results which are too low by 3 to 4 orders of magnitude and that their law is not correct in general.

At the present time the most widely accepted theory is that of Keywell,⁵ which is based on the technique proposed by Seitz²⁰ for computing the number of displaced atoms, but which was developed only for energies up to 5 – 6 keV. We have therefore attempted to establish a relationship between the number of displaced atoms and the number of atoms sputtered by a single incident hydrogen or deuterium ion in the energy range 0.6 keV – 10 MeV. Data on the proton-stopping power of copper were taken from reference 21 and were extrapolated to the 0.6 – 6 keV region. The stopping power for deuterons was computed from Warshaw's data²² for protons with the same velocities as the deuterons. Figures 7 and 8 show the results of the computations and preliminary runs, which indicate that about 5% of the displaced copper atoms are sputtered in the entire investigated energy range.

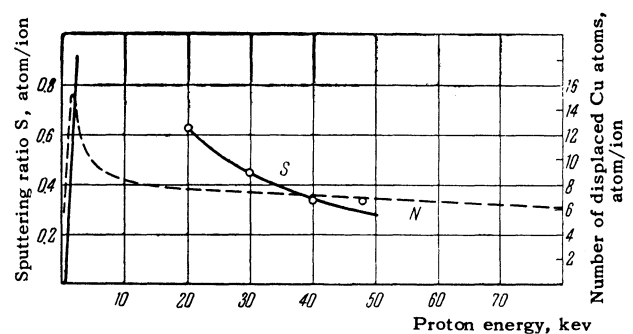


FIG. 8. Comparison of the number of displaced copper atoms with the number of sputtered atoms produced by protons up to 100 keV.

It is necessary to discuss the possible experimental errors. The composition of the beam was

known only very approximately because of the lack of a mass-spectrographic analysis. The beam included nitrogen and oxygen ions, resulting from charge exchange with hydrogen ions, which were able to induce additional sputtering; we shall now estimate the corresponding error. The charge-exchange cross sections for these vapors have been thoroughly investigated by a number of authors (see reference 23, for example) and the value $\sim 5 \times 10^{-16}$ cm² has been obtained for the maximum at 5 keV. In the univoltage electrostatic lens the mean free path of ions with this energy did not exceed 6–8 cm. It was easily computed that under the given working conditions N₂⁺ and O₂⁺ could not comprise more than 1% of the total beam current. This was confirmed experimentally by Orfanov,²⁴ who studied the mass spectrum of a beam in a similar gun. Under the given operating conditions of the ion source the beam was found to consist of H₂⁺ (40–50%), H₁⁺ (30–40%), H₃⁺ (30–10%), N₂⁺ and O₂⁺ (1–3%). The sputtering ratio of copper by nitrogen ions is 2 atom/ion.¹¹ Therefore N₂⁺ and O₂⁺ should not produce an error greater than 6–10% in the value of S for hydrogen ions.

The author is deeply indebted to Professor B. K. Shembel' for suggesting this research and for his continued interest. He is also indebted to D. V. Karetnikov, S. N. Popov, I. F. Kvartskhava, and P. P. Dmitriev, who made it possible to perform the experiments using the ion gun and the cyclotron.

The author wishes to thank V. I. Lisovskii for assistance in preparing and conducting some of the experimental runs; I. N. Slivkov for valuable discussions; and Professor N. D. Morgulis and M. I. Guseva for discussions of the results.

¹L. N. Dobretsov and N. M. Karnaukhova, Dokl. Akad. Nauk S.S.S.R. **85**, 745 (1952).

²M. A. Eremeev and Ya. K. Éstrinov, J. Tech. Phys. (U.S.S.R.) **22**, 1552 (1952).

³R. Bradley, Phys. Rev. **93**, 719 (1954).

⁴F. Fairbrother and J. S. Foster, Vacuum **4**, 112 (1954).

⁵F. Keywell, Phys. Rev. **97**, 1611 (1955).

⁶J. R. Young, J. Appl. Phys. **26**, 1302 (1955).

⁷L. V. Zyrina and M. D. Yagudaev, Tr. Sredneaziat'skogo universiteta (Trans. Central Asia University) **65**, 33 (1955).

⁸M. I. Guseva, Приборы и техника эксперимента (Instrum. and Meas. Engg.) **5**, 112 (1957).

⁹Moore, O'Briain, and Lindner, Ann. N.Y. Acad. Sci. **67**, 600 (1957).

¹⁰R. E. Honig, J. Appl. Phys. **29**, 549 (1958).

¹¹Rol, Fluit and Kistemaker, Terzo congresso internazionale sui fenomeni d'ionizzazione nei gas tenuto a Venezia dall' 11 al 15 giugno, Milano, 1957.

¹²M. Ardenne, Tabellen der Elektronenphysik, Ionenphysik und Übermikroskope, Berlin, 1956; Technik **2**, 3 (1956).

¹³D. V. Karetnikov, Dissertation, Inst. Chem. Phys., Acad. Sci. U.S.S.R., 1954; Egorov, Karetnikov and Popov, Приборы и техника эксперимента (Instrum. and Meas. Engg.) in press.

¹⁴L. P. Khavkin, J. Tech. Phys. (U.S.S.R.) **26**, 2356 (1956), Soviet Phys.-Tech. Phys. **1**, 2279 (1956).

¹⁵A. Guntherschulze and K. Meyer, Z. Physik **62**, 607 (1930).

¹⁶A. E. Ennos, Brit. J. Appl. Phys. **4**, 101 (1953); **5**, 27 (1954).

¹⁷R. Seeliger and K. Sommermeyer, Z. Physik **93**, 692 (1935).

¹⁸A. Guntherschulze, Z. Physik **119**, 79 (1942).

¹⁹D. T. Goldman and A. Simon, Bull. Am. Phys. Soc. Ser II, **3**, 40 (1958); Phys. Rev. **111**, 383 (1958).

²⁰F. Seitz, Discussions Faraday Soc. **5**, 271 (1949).

²¹H. Batzner, Ann. Physik **25**, 233 (1938).

²²S. D. Warshaw, Phys. Rev. **76**, 1759 (1949).

²³P. M. Stier and C. F. Barnett, Phys. Rev. **103**, 896 (1956).

²⁴I. V. Orfanov, Report Inst. Chem. Phys., Acad. Sci. U.S.S.R., 1959.